Numerical Simulation of Hypersonic Blunt Body and Nozzle Flows using Master Equation

Prakash Vedula* and Eswar Josyula†

*School of Aerospace and Mechanical Engineering, University of Oklahoma, Norman, Oklahoma, U.S.A.
†Air Force Research Laboratory, Wright-Patterson AFB, Ohio, U.S.A.

Abstract. Numerical simulations of hypersonic flow past blunt body and expanding nozzles were conducted using an operator splitting approach for coupling the master equation consisting of state-to-state kinetics with the fluid dynamic equations. The vibrational-translational (V-T) and vibrational-vibrational (V-V) energy transfer processes were included in the master equation. The resulting stiff system of equations were solved satisfactorily with the operator splitting approach. Separate nozzle simulations were performed with pure nitrogen and pure oxygen in the temperature ranges of 5000 K – 6000 K and 2200 K – 3500 K, respectively. Highly nonequilibrium (i.e. non-Boltzmann) distributions were predicted at the nozzle exit for the selected range of temperatures. The contribution of vibrational-vibrational (V-V) transition rates to the overall vibrational relaxation process was found to be higher at the lower nozzle throat temperatures.

Keywords: Continuum, Nonequilibrium, Hypersonic flow, State-Kinetic Rates, Master Equation, Operator Splitting
PACS: 47.45.Ab,47.40.Ki

INTRODUCTION

Proper treatment of energy transfer between nonequilibrium molecular energy modes is important for the prediction and understanding of the aerothermodynamics of gas systems, viz. aerodynamic heating on hypersonic vehicles and thrust in propulsive nozzles [1]. At re-entry conditions where the gas temperature is very high, molecular collisions result in the exchange of the translational, rotational, vibrational, and electronic energies of the collision partners. The probabilities or effective cross sections of these elementary processes differ significantly, giving rise to large differences in relaxation times for the internal modes. Thus it is important to account for the rates of relaxation processes to accurately predict the nonequilibrium behavior.

The nonequilibrium conditions behind the shock wave of a blunt body exemplify the case where the translational temperature, T, is greater than the vibrational temperature, T_v,ultimately approaching near-equilibrium conditions close to the surface of the body [2]. In expanding nozzle flows, however, the effect of vibration-dissociation coupling on the vibrational population density is reversed and the population is enhanced. The sonic flow at the inlet of the nozzle is in thermal equilibrium and as the flow proceeds towards the exit of the nozzle, the flow departs from the equilibrium conditions. The vibrational temperature freezes near the inlet and the translation temperature rapidly falls as a result of the expansion process [3].

Vibrational relaxation involves two separate time scales, associated with (i) the exchange of energy between vibrational and translational modes (V-T exchange) and (ii) the exchange of energy among vibrational-vibrational modes (V-V exchange). The fact that the time scales, $\tau_{V-V} << \tau_{V-T}$, are far enough apart allows one to segregate fast and slow time scales associated with a process. During the fast stage, V-V exchanges dominate the kinetics and during the slow stages the V-T transfers dominate. The distribution of energy among various vibrational quantum energy levels is modeled based on an anharmonic oscillator model.

The nonequilibrium vibrational energy distribution is modelled by the master equation to calculate the population distributions by considering the kinetics of particle exchanges among the quantum states. In the earlier work of Casual, et ale [4] the vibrational master equation was coupled to fluid dynamic equations to assess the role of the V-T and V-V energy transfers on the hypersonic flowed. In this approach, each quantum energy state is represented by a separate conservation of mass equation. Obtaining numerical solutions of the underlying governing equations can be very challenging due to the extreme stiffness of the system where the physical phenomena due to transport and collisions (via master equations) occuring across multiple time scales are strongly coupled. Direct representation of such strongly coupled physical processes spanning a wide range of time scales imposes stringent restrictions on the maximum allowable time step that can be used in the numerical simulation. While the maximum time step needed

for numerical stability is governed by the Courant-Freidrich-Levy (CFL) number for numerical representation of pure advection processes, the constraints due to stiffness of the master equations (based on eigenvalue analysis) results in a time step estimate that is much smaller than that given the CFL criterion (for pure advection). To alleviate the underlying computational costs, it is possible to use a separate numerical treatment for each of the underlying physical processes, where the time steps chosen in the evolution of the state variables during each of those physical processes are selected based on the underlying characteristic time scales.

In this paper, we propose the use of an operator splitting formalism to address some challenges associated with the time step limitations of the previously studied strong coupling forms. In the current work, transport and collision term (via the master equation) are handled using the operator splitting approach. In this approach, the advection equation and master equation are separately solved and the numerical time integration step needed along the evolution of each physical process is selected based on its underlying individual requirement. The evolution operator is split into operators corresponding to transport and collision (due to master equation). The operator for transport is numerically handled using standard CFD techniques, where the the operator corresponding to collisions is handled via a stiff ordinary differential equations (ODE) integration solver. The maximum time step needed for the transport step is governed by the CFL criterion where as the time step needed by the stiff ODE solver depends on the tolerances used for satisfying the convergence criteria. The former time step due to the transport processes is often much larger than the latter time step (used in the master equation). This is in contrast with the earlier strong coupling form where the smallest of the two time steps has to be used, which in turn results in a higher computational cost (and often impractical to consider) compared to the proposed operator split formalism.

In order to verify the code and validate our results based on operator splitting approaches, we compare the results with those obtained based on strong coupling for a Mach 6.5 nitrogen flow past a blunt body. To further test the operator splitting approach for stiff systems, the present work simulates hypersonic flow in expanding nozzle where the widely varying rates of V-T and V-V energy transfer rates are considered. The flow in a high temperature nozzle flow of nitrogen flow with nozzle throat temperatures of 5000 K and 6000 K are considered. And an oxygen flow in a nozzle is considered for the nozzle throat temperatures of 2200 K, 2700 K, and 3500 K. The fluid dynamic equations coupled to the master equations including the V-T and V-V processes are solved to delineate the various kinetic processes occuring in the nozzle.

ANALYSIS

The global conservation equations in mass-averaged velocity form to simulate hypersonic flow are presented in this section. The models used to simulate the V-T and V-V processes are then discussed.

$$\partial_t(\rho_v) + \nabla \cdot (\rho_v \vec{\mathbf{u}}) = \dot{\omega}_v \quad v=0,1,... \tag{1}$$

$$\partial_t(\rho \vec{\mathbf{u}}) + \nabla \cdot (\rho \vec{\mathbf{u}}\vec{\mathbf{u}} - p\overline{\overline{\delta}}) = 0 \tag{2}$$

$$\partial_t(\rho e) + \nabla \cdot [\rho(e + p/\rho)\vec{\mathbf{u}}] = 0 \tag{3}$$

Equations (1) to (3) describe the conservation of mass, momentum and energy in the flowfields of interest, where ρ and ρ_v denote the total mass density and mass density of a vibrational state v respectively. The symbols $\mathbf{u}$, p and e denote the velocity vector, pressure and total energy per unit mass respectively. Equation (1) is discussed further in the following section. Equations (2) and (3) represent the conservation of total momentum and energy, respectively. A microscopic kinetic approach was taken by treating the molecule as anharmonic oscillator, calculating the state populations using the master equations. In the treatment of vibrational energy for the diatomic species in the master equation code, a separate vibrational conservation equation is not necessary as the vibrational energy can be calculated for each quantum level.

The conservation equation for the mass density in a quantum level v is given by Eq. (1) is written for the mass. The source term $\dot{\omega}_v$ derived from the vibrational master equations is made up of the relevant energy exchange processes consisting of the V-T and V-V processes. The mass density of the molecular species is the sum of the corresponding state densities in the vibrational levels, as $\rho = \sum_{v=0}^{v^*} \rho_v$. The symbolic equations governing the V-T transitions responsible for the variation of the particles distributed in the v^{th} vibrational level are: $N_2(v) + N_2 \rightleftharpoons N_2(v') + N_2$ and the equations governing the V-V process are: $N_2(v) + N_2(w) \rightleftharpoons N_2(v') + N_2(w')$, where v, w, v' and w' denote different vibrational quantum num numbers.

The kinetics of the particle exchanges among the quantum states are simulated using the vibrational master equations (along with anharmonic oscillator models), where the population distributions are calculated with [4]:

$$\dot{\omega}_v = \frac{1}{\mathscr{M}}\{\sum_{v'}[k_{VT}(v' \rightarrow v)\rho_{v'}\rho - k_{VT}(v \rightarrow v')\rho_v\rho] + \sum_{w,v',w'}[r_{VV}(v',w' \rightarrow v,w)\rho_{v'}\rho_{w'} - r_{VV}(v,w \rightarrow v',w')\rho_v\rho_w]\} \tag{4}$$

In the present calculations, the energy exchanges consist of multi-quantum transitions for VT and VV processes. The VT process is associated with the rate coefficient k_{VT} where the molecule loses or gains number of vibrational quanta. The de-excitation rate from v' to v for colliding molecules is denoted by $k_{VT}(v' \rightarrow v)$, the inverse collision from $v \rightarrow v'$ by $k_{VT}(v \rightarrow v')$. When considering VV exchanges, the initial and final vibrational states of each collision partner must be identified; thus the transition rate from v' to v and w' to w is given by $r_{VV}(v',w' \rightarrow v,w)$. Consistency of the rate coefficient with the principle of detailed balance is enforced.

Numerical Method

In this section we describe the numerical implementation of the governing equations, where the conservation of mass equation is treated with and without operator splitting. In order to describe the method, we write the governing equations, Eq. (1) – (3), in a convenient form as: $\partial_t \mathbf{U} + \nabla \cdot \mathbf{F} = \mathbf{H}$, where the vector $\mathbf{U}$ is given by $\begin{bmatrix}\rho_0 & \rho_1 & \dots & \rho_{\mathscr{N}} & \rho u & \rho v & \rho e\end{bmatrix}^T$. Similarly $\mathbf{F}$ and $\mathbf{H}$ can also be written out from Eq. (1)–(3). In the non-split approach that we refer to as strong coupling form, a predictor-corrector based numerical method is used to achieve 2nd order spatial and temporal accuracy. The Roe approximate Riemann solver is used to determine the inviscid fluxes. Formal 2nd order accuracy is obtained using the MUSCL approach in conjunction with the *minmod* limiter to degenerate the solution to first order accuracy in the vicinity of strong waves. [5, 6]

Numerical solution of the underlying governing equations can be quite challenging especially due to high computational costs, arising not only due to many degrees of freedom but also due to inherent stiffness of the governing differential equations. Numerical solutions involving a strong coupling of convection processes with state-to-state transitions (via master equations) often lead to stiff systems that are difficult to solve. For time dependent problems, this difficulty can lead to the use of a needless and unreasonably small time step for both transport and kinetics. To alleviate this difficulty, operator splitting methods can be used where the solution is split into separate integrations for (i) physical transport and (ii) state-to-state kinetics. Such operator splitting methods allow for separate time steps can be used for each of these two integration stages. Numerical integration of physical transport operator is done using a standard second-order Runge-Kutta scheme, where as the state-to-state kinetics are handled using a stiff solver for ordinary differential equations (such as DLSODA). Such operator splitting approaches (e.g. Strang splitting) [7, 8, 9] have been widely used in computational combustion, where the complete evolution operator is split into for physical transport and stiff chemistry. It can be shown that operator splitting introduces an error which can be alleviated with a proper ordering of the operators.

To better describe the operator splitting approach, we denote the evolution operator accounting for both transport and collisions (via Master equation) over time step Δt as $\Phi^{\Delta t}$ corresponding to the governing equations (as described above). Based on this evolution operator, the state vector $\mathbf{U}$ at time $t + \Delta t$ (denoted at $\mathbf{U}^{t+\Delta t}$) can be expressed as, $\mathbf{U}^{t+\Delta t} = \Phi^{\Delta t}\mathbf{U}^t$.. Instead of directly seeking numerical approximations of the operator Φ which accounts for the effects of both transport and collision operators, we use an operator split formalism where the state vector at $\mathbf{U}$ at time $t + \Delta t$ can be expressed as

$$\mathbf{U}^{t+\Delta t} = \Phi_C^{\Delta t/2}\Phi_T^{\Delta t}\Phi_C^{\Delta t/2}\mathbf{U}^t, \tag{5}$$

where Φ_T and Φ_C denote evolution operators due to pure transport and pure collision processes (master equation) corresponding to the following system of equations.

$$\Phi_T : \qquad \partial_t \mathbf{U} + \nabla \cdot \mathbf{F} = 0 \tag{6}$$

$$\Phi_C : \qquad \partial_t \mathbf{U} = \mathbf{H} \tag{7}$$

This operator split formalism, consistent with original formulation by Strang [9], can be shown to be second order accurate in time. Based on the above operator split formalism, we further approximate the operators Φ_T and

Φ_C. The former is treated numerically similar to the non-split case (except that source term $\mathbf{H} = 0$ for the pure transport step) discussed earlier, where a second order accurate predictor-corrector method with Roe upwind difference scheme is used. While the evolution operator for collisions Φ_C (given by the master equation) is treated via a stiff ordinary differential equation (ODE) integration solver. The present study utilizes the DLSODA stiff ODE integration package [10].

RESULTS AND DISCUSSION

Results showing the verification of the CFD method are presented first, followed by the numerical simulations of highly nonequilibrium hypersonic expanding flow in a nozzle. Code verification is conducted by comparing results from the current splitting method with the strong coupling method [4, 2] for a Mach 6.5 nitrogen flow past a 1-meter diameter 2D cylinder. Figure 1 shows the temperature profiles along the stagnation streamline and along the surface, respectively. The translational and first level vibrational temperature profiles have excellent agreement. These results also agree with the work of Giordano, et al. [11]. For this flow, the translational and vibrational temperatures are set to 300 K in the freestream. Across the shock wave, the translational temperature rises by a factor of 10 along the stagnation streamline and remains close to this value in the shock layer. The vibrational energy manifold is heated in the shock layer, primarily by the V-T energy transfers and approaches the translational temperature at the stagnation point. Along the surface the translational temperature is the highest at the stagnation point and undergoes a sharp decrease compared to the vibrational temperature. The L_2 norm of the error, $\tilde{e} \equiv \lim_{t\to\infty} \|\mathbf{U}(t+\Delta t) - \mathbf{U}(t)\|$ was computed to monitor convergence. The time evolution of the L_2 norm from the current splitting method is shown in figure 1 The figure shows the L_2 norm for two cases, (1) where the vibrational relaxation is treated with V-T energy transfers alone, and (2) the vibrational relaxation consists of V-T and V-V energy transfers. The L_2 norm for both cases, decreases to less than 1.0e-07, the effect of V-V energy transfers showing a lower value at all times.

The nozzle experiments conducted in the NASA Ames EAST facility by Gillespie et. al [12] were numerically simulated by Josyula and Bailey [3] on a computational grid that was a quasi one-dimensional adaptation of the two-dimensional nozzle. The area ratios of the quasi one-dimensional adaptation of Ref.[12] were used in the present study to generate the nozzle grid for the numerical studies. The temperature distribution a reservoir temperature, T_0=5600 K, is presented in Fig. 2. Two experimental measurements at each location are shown. Experimental error bars for the data [12] is shown for only two data points near the exit of the nozzle. Similar error can be expected at other data points in the nozzle as well. For this case, vibrational temperature predictions using the Millikan and White rates, provide the best match with data. The current FHO rates yield lower vibrational temperatures than those of Millikan and White. Although, the state-to-state kinetic rates were used in a master equation approach, the minor role of V-V rates and anharmonicity makes the solution highly dependent on the V-T rate of the first excited state. As pointed out earlier [3], the magnitude of the V-T de-excitation rates, k_{10} are important in the accurate prediction of the nozzle flowfield. An additional simulation was conducted for a higher nozzle throat temperature of 6000 K to assess the effect of V-V energy transfers. The degree of nonequilibrium for the two temperatures is also shown in Fig. 2. It is seen that equilibrium conditions prevail at the throat and the degree of nonequilibrium increases with the flow and is the highest at the exit of the nozzle. The effect of V-V energy transfer, Fig. 2, is highlighted by population distributions in the quantum energy states in the vibrational manifold. The population distributions at the throat location show Boltzmann distributions. Those at the exit of the nozzle depict non-Boltzmann distributions, the effect of V-V transfer is more pronounced at the lower throat temperature of 5000 K. The evolution of the L_2 norm for the two methods for the T_{throat}=5000K case, with reference strong coupling and the current splitting approaches, is shown in Fig. 3. The L_2 norm of the current splitting method is lower by about an order of magnitude and is less oscillatory. The effect of V-V energy transfers on the L_2 norm is also shown in Fig. 3. It is noted that unlike the blunt body case, the effect of V-V energy transfers has a higher L_2 norm at the steady state conditions.

Expanding nozzle flow simulations of oxygen are discussed in this section for three throat temperatures, 2200 K, 2700 K, and 3500 K to assess the affect of the V-V energy transfer process on the flow. In all three cases, the vibrational temperature freezes slightly downstream from the throat and the translational temperature shows a steady decrease along the length of the nozzle. It is noted that the degree of nonequilibrium for the T_{throat}=2200 K is the highest, and the degree of nonequilibrium decreases with increasing throat temperature. The degree of nonequilibrium is further highlighted in Fig. 4.

The effect of V-V energy transfers are shown for these cases in Fig. 4. The population distributions at the throat are shown to follow the Boltzmann distribution. However, the effect of V-V energy transfers is the highest for the case of T_{throat}=2200 K (Fig. 4). The effect of V-V energy transfers decreases with increase in nozzle throat temperature and

for T_{throat}=3500 K, the effect of V-V energy exchanges is the lowest (among the cases considered).

CONCLUDING REMARKS

An operator splitting algorithm was implemented to couple the master equation with the fluid dynamic equations to solve the coupled set of a stiff system of equations for highly nonequilibrium flowfields for non-reactive hypersonic conditions. The master equation consists of vibration-translation (V-T) and vibration-vibration (V-V) energy transfer processes with detailed state-to-state kinetics. Detailed flowfield solutions for hypersonic flows in thermal nonequilibrium were performed where the fluid dynamic equations were solved by coupling them to the vibrational master kinetic equations for 47 quantum levels of the nitrogen molecule and the 30 quantum levels of the oxygen molecule, assumed as anharmonic oscillator.

Verification and validation of the operator splitting approach was conducted with results from the strong coupling approach. There was excellent agreement between the two approaches. The operator splitting approach was used to solve the expanding nozzle flows for two diatomic gases, one with pure nitrogen and the other with pure oxygen. The nozzle with nitrogen was simulated for two throat temperatures of 5000 K and 6000 K. The nozzle with oxygen was simulated for three throat temperatures of 2200 K, 2700 K, and 3500 K. For both the cases, highly non-Boltzmann distributions were predicted at the nozzle exit and the influence of V-V rates on the V-T rates was higher at the lower nozzle throat temperatures.

Support for EJ was provided by the U.S. Air Force Office of Scientific Research contracts monitored by F. Fahroo.

REFERENCES

1. J. Rich, S. Macheret, and I. Adamovich, *Experimental Thermal and Fluid Science* **13**, 1–10 (1996).
2. E. Josyula, and W. Bailey, *AIAA Paper 2005-5204* (2005).
3. E. Josyula, and W. Bailey, *AIAA Paper 2002-0200* (2002).
4. E. Josyula, *Journal of Thermophysics and Heat Transfer* **14**, 18–26 (2000).
5. E. Josyula, D. Gaitonde, and J. Shang, *AIAA Journal* **31**, 812–813 (1993).
6. R. Walters, P. Cinnella, and D. Slack, *AIAA Journal* **30**, 1304–1313 (1992).
7. O. M. Knio and H. N. Najm and P. S. Wyckoff, *J. Computational Physics* **154**, 428–467 (1999).
8. Z. Ren and S. B. Pope, *J. Computational Physics* **227**, 8165–8176 (2008).
9. G. Strang, *SIAM J. Numerical Analysis* **5**, 506–517 (1968).
10. A. Hindmarsh, "ODEPACK: A Systematized Collection of ODE Solvers," in *Scientific Computing*, North-Holland, Amsterdam, 1983, pp. 55–64.
11. D. Giordano, V. Bellucci, G. Colonna, M. Capitelli, I. Armenise, and C. Bruno, *Journal of Thermophysics and Heat Transfer* **11**, 27–35 (1997).
12. W. Gillespie, D. Bershader, S. Sharma, and S. Ruffin, *AIAA Paper 93-0274* (1993).

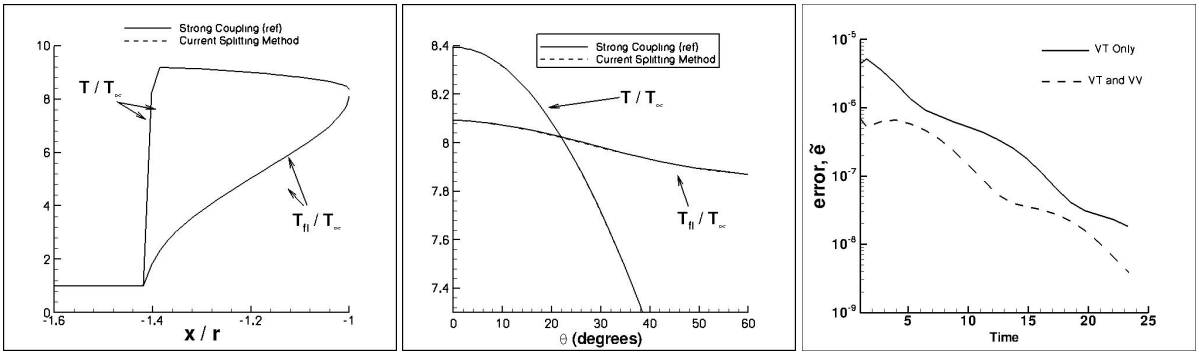

FIGURE 1. Code verification: Translational and vibrational temperatures along the stagnation streamline (left) and along the surface (center) for nitrogen flow past blunt body, M_∞=6.5, r=1 m, T_∞=300 K, Tv_∞=300 K, p_∞=50 Pa. Comparison of L_2 norm of error, $\tilde{e}$, for source term splitting formulation for (i) VT only and (ii) VT & VV exchanges, with 10, 20, and 40 vibrational quantum levels of nitrogen is shown on the rightmost figure.

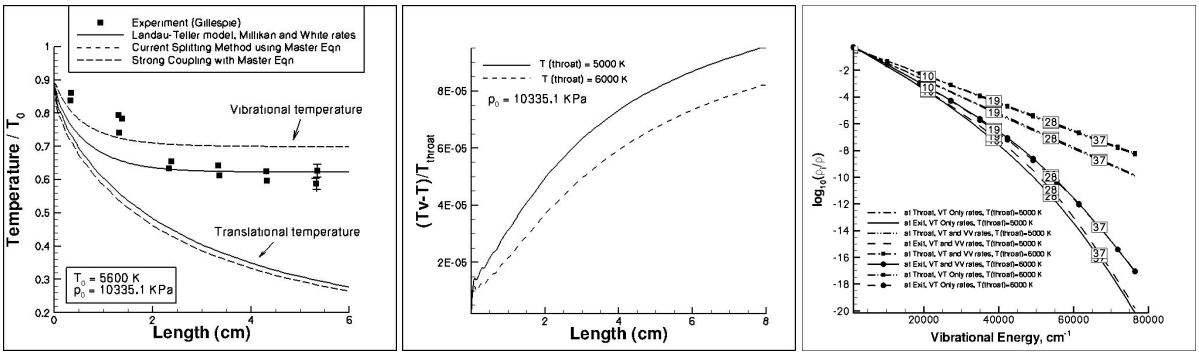

FIGURE 2. (Left) Comparison with experiment: temperatures along centerline of nozzle, $T_0 = 5600\ K$, $p_0 = 10335.1kPa$, Medium=N_2. (Center) Degree of nonequilibrium for different throat temperatures, $p_0 = 10335.1kPa$. (Right) Population distributions along centerline, (a) throat and (b) exit of nozzle, $T_0 = 5600\ K$, $p_0 = 10335.1kPa$.

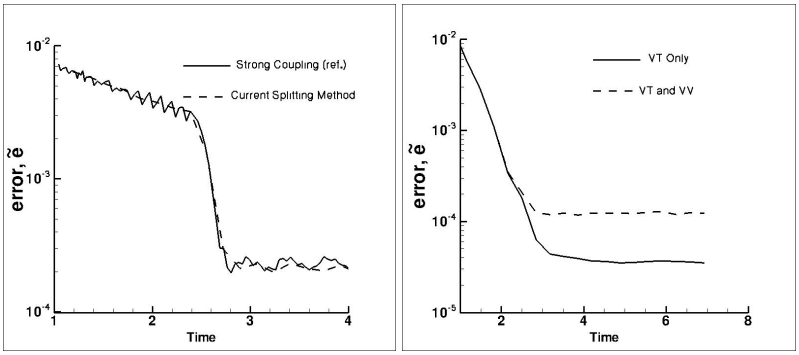

FIGURE 3. Comparison of L_2 norm of error, $\tilde{e}$ with 40 vibrational quantum levels for N_2: (Left) for (a) Strong Source Term Coupling and (b) Source Term Splitting, T_{throat}=5,000 K, and (Right) for source term splitting formulations of (a) VT Only and (b) VT & VV energy exchanges, T_{throat}=6000 K

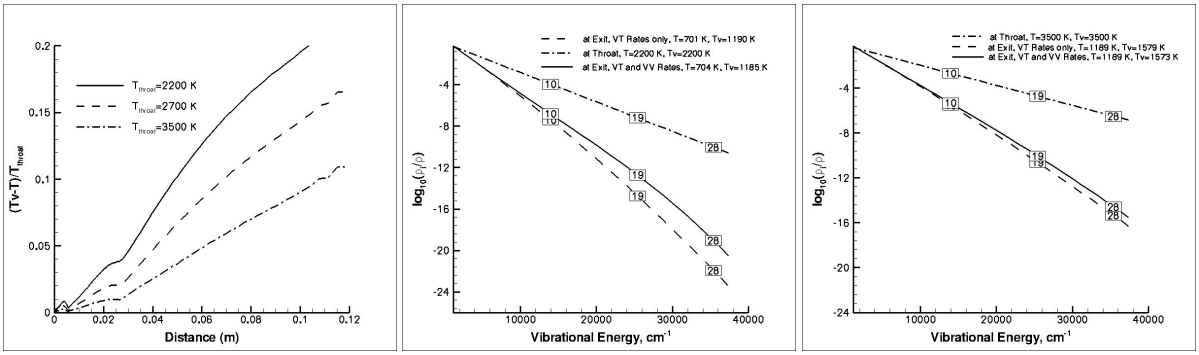

FIGURE 4. (Left) Degree of nonequilibrium for different throat temperatures, $p_{throat} = 6816kPa$, Medium=O_2. Population distributions along centerline, at (i) throat and (ii) exit of nozzle, for $T_{inlet} = 2200\ K$ (center) and $T_{inlet} = 3500\ K$ (right) are also shown.